ANALYTICAL AND EXPERIMENTAL PARAMETER ESTIMATION FOR FREE-FLOATING SPACE MANIPULATOR SYSTEMS

Olga-Orsalia Christidi-Loumpasefski, Christos Ntinos, Evangelos Papadopoulos

National Technical University of Athens
School of Mechanical Engineering – Control Systems Laboratory
9 Heroon Polytechneiou Str., 15780, Athens, Greece
Email: {olgaloumpasefski, christos.ntinos93}@gmail.com, egpapado@central.ntua.gr

ABSTRACT

The use of Space Manipulator Systems (SMS) is currently an important element of space missions. In order for an SMS to accomplish the necessary tasks efficiently and accurately, advanced model-based control methods need to be employed. These methods require accurate knowledge of the system's dynamic parameters, whose values are very often unknown or subject to change on orbit for a number of reasons, such as fuel consumption, deployment of payloads, docking to a spacecraft, or object capture. In this paper, a novel method for parameter identification of a free-floating robotic space manipulator system is proposed based on the conservation of the angular momentum. Moreover, the NTUA's new planar space emulator is presented. The proposed identification method is validated by a numerical simulation and subsequently it is used for the experimental identification of NTUA's space emulator.

1. INTRODUCTION

Successes in space exploration have emphasized the growing importance of On-Orbit Servicing (OOS) in space programs around the world. OOS includes missions, such as re-orbiting and de-orbiting, inspection and retrofitting of orbiting structures, satellite maintenance, satellite repair, and removal of space debris. A cost-effective way to accomplish these is to use space manipulator systems (SMS), see "Fig. 1", since space conditions are too dangerous to human life, especially during EVAs.

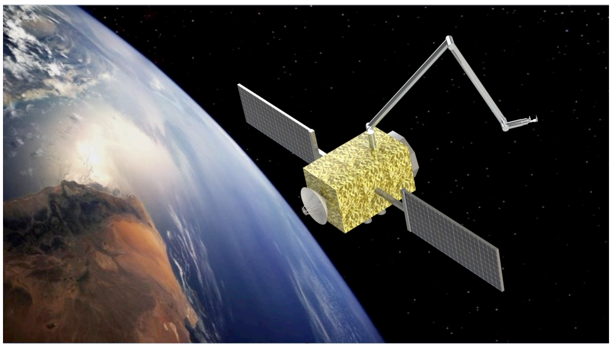

Figure 1. Space Robotic System in Free-Floating Mode.

An On Orbit Servicing mission, particularly important for the future of operations in space, is the active removal of space debris. The high number of satellites placed on orbit over the past 50 years, has resulted in a great number of space debris endangering the success of current and future missions. Moreover, collisions between existing debris result in numerous new space debris, potentially leading to a chain that is estimated to render certain orbits non-operational in the near future.

The first documented accidental hypervelocity collision between two intact artificial satellites in low Earth orbit took place in 2009. The collision occurred between the deactivated Russian military communication satellite Cosmos 2251 and the active commercial US-built satellite Iridium 33. As of August 2009 the US Space Surveillance Network (SSN) has catalogued 386 pieces of debris (16 pieces of which have already decayed from orbit) associated with Iridium 33 and 927 pieces of debris (30 pieces of which have decayed) associated with Cosmos 2251 [1].

The incidents described above, illustrate in the best way possible the urgent need for Active Debris Removal (ADR) missions. As part of such mission, numerous designs have been proposed for chaser-spacecraft equipped with tentacles, nets, harpoon mechanisms and more, as well as contactless methods such as electrostatic and gravity tractors [2]. One of the most promising active debris removal methods is the deployment of robotic systems with one or more manipulators. These systems are designed to be able to track and make contact with a potentially uncooperative target-debris, which will then be removed from its orbit and burned through in the upper atmosphere.

Beyond their potential service in the active debris removal missions, an SMS is expected to be useful in other aspects of OOS such as repairs and construction on orbit. Thus, intelligent systems are required in order to complete these highly complicated tasks successfully.

The tasks being performed as part of an OOS mission can benefit substantially from the accurate knowledge of the dynamic parameters of the servicing system as well as those of the target, since the high precision required can only be achieved by the implementation of advanced model based control strategies. Therefore, the need for parameter identification methods arises.

Many parameter estimation methods have been developed, inspired by methods for fixed-base manipulators, [3], [4], and based on the linearity of the equations of motion with respect to the dynamic properties of the system, [5], [6]. However, these methods require measurements of spacecraft angular acceleration and joint accelerations, which contain undesirable noise and torque measurements, hard to obtain. To address this issue, some researchers have proposed, in the case of a free floating SMS (FFSMS), the use of estimation algorithms based on the conservation of angular momentum, [7], [8], [9]. These methods, however, fail to estimate all the dynamic parameters of the system without the prior knowledge of some of them. In this paper a novel parameter method is implemented, which is based on the conservation of angular momentum and renders the system's dynamics fully identified [10]. The method is used for the theoretical and experimental parameter identification of NTUA's robotic space emulator.

2. PARAMETER IDENTIFICATION METHOD BASED ON THE CONSERVATION OF ANGULAR MOMENTUM

Advanced control strategies for FFSMS use the Generalized Jacobian matrix and the dynamic model of the system; hence they need knowledge of the system parameters, [11]. To this end, we present the angular momentum equation of an FFSMS with multiple manipulators and zero external forces and torques. We assume that the system has constant angular momentum, and without loss of generality, zero linear momentum, [12]. The FFSMS have an open chain kinematic configuration consist of n manipulators. The number of the links of the m-th manipulator is indicated by N_m. Under these conditions, the system Center of Mass (CM) remains fixed in inertial space, and hence the origin of an inertial frame, O, can be chosen to be the system CM, see "Fig. 2".

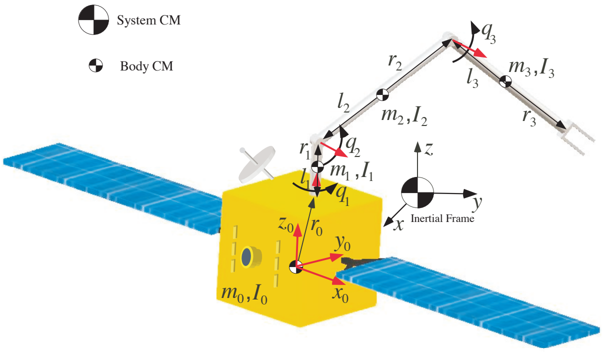

Figure 2. A spatial FFSMS and the definition of its parameters.

The system angular momentum expressed in the inertial frame is given by:

$$\mathbf{h}_{CM} = \mathbf{R}_0 ({}^0\mathbf{D}\, {}^0\boldsymbol{\omega}_0 + {}^0\mathbf{D}_q \dot{\mathbf{q}}) \tag{1}$$

where ${}^0\boldsymbol{\omega}_0$ is the spacecraft angular velocity expressed in the spacecraft 0^{th} frame and the column-vector $\dot{\mathbf{q}}$ is:

$$\dot{\mathbf{q}} = [\ \dot{\mathbf{q}}^{(1)\mathrm{T}} \quad \cdots \quad \dot{\mathbf{q}}^{(m)\mathrm{T}} \quad \cdots \quad \dot{\mathbf{q}}^{(n)\mathrm{T}}\ ]^{\mathrm{T}} \tag{2}$$

where the $N_m \times 1$ column-vector $\dot{\mathbf{q}}^{(m)}$ represents the joint rates of the m-th manipulator. The matrix $\mathbf{R}_0(\boldsymbol{\varepsilon},\eta)$ is the rotation matrix between the spacecraft 0^{th} frame and the inertial frame, expressed as a function of the Euler parameters $\boldsymbol{\varepsilon},\eta$, and the terms ${}^0\mathbf{D}, {}^0\mathbf{D}_q$ are inertia-type matrices of appropriate dimensions, given in APPENDIX A.

To use Eq. 1 for parameter estimation, the angular momentum $\mathbf{h}_{CM}$ must be expressed linearly with respect to the vector of the estimated parameters $\boldsymbol{\pi}$. Thus, the angular momentum can be expressed as:

$$\mathbf{h}_{CM} = \mathbf{Y}(\dot{\mathbf{q}}, \mathbf{q}, {}^0\boldsymbol{\omega}_0, \boldsymbol{\varepsilon}, \eta)\boldsymbol{\pi} \tag{3}$$

where the $3 \times k$ matrix $\mathbf{Y}$ is the regressor matrix.

Assuming constant angular momentum $\mathbf{h}_{CM,0}$, and N measurements of the variables $\dot{\mathbf{q}}, \mathbf{q}, {}^0\boldsymbol{\omega}_0$ and $\boldsymbol{\varepsilon},\eta$ obtained at time instants $t_1, t_2, ..., t_N$ during an appropriate trajectory, results in the following system of equations:

$$\hat{\mathbf{h}}_{CM} = \begin{bmatrix} \mathbf{h}_{CM,0} \\ \mathbf{h}_{CM,0} \\ \vdots \\ \mathbf{h}_{CM,0} \end{bmatrix} = \begin{bmatrix} \mathbf{Y}(t_1) \\ \mathbf{Y}(t_2) \\ \vdots \\ \mathbf{Y}(t_N) \end{bmatrix} \boldsymbol{\pi} = \hat{\mathbf{Y}}\boldsymbol{\pi} \tag{4}$$

Appropriate exciting trajectories must be followed by the manipulators. These exciting trajectories are required to result in $\mathbf{Y}$ being of full rank and with a small condition number. A small condition number is needed so that the estimation is relatively insensitive to measurement noise.

The number of the measurements N should satisfy Eqs. 5-6 for spatial and planar free-floating space robots, respectively,

$$3N \geq k \tag{5}$$

$$N \geq k \tag{6}$$

The vector $\boldsymbol{\pi}$ should contain the minimum set of estimated parameters so that the regressor $\hat{\mathbf{Y}}$ is of full rank. Therefore, a case-by-case analysis is required. Suppose that initially the $\mathbf{Y}$ and $\boldsymbol{\pi}$ are:

$$\mathbf{Y} = \begin{bmatrix} \mathbf{e_1} & \cdots & \mathbf{e_i} & \cdots & \mathbf{e_k} \end{bmatrix} \tag{7}$$

and

$$\boldsymbol{\pi} = \begin{bmatrix} \pi_1 & \cdots & \pi_i & \cdots & \pi_k \end{bmatrix}^{\mathrm{T}} \tag{8}$$

where $\mathbf{e_i}$ is the i^{th} column of matrix $\mathbf{Y}$ and π_i is the i^{th} element of column vector $\boldsymbol{\pi}$. To find the minimum set of parameters, one must examine if a column $\mathbf{e_i}$ can be written as a linear combination of the other columns, i.e.,

$$\mathbf{e_i} = \sum_{j=1,\ j\neq i}^{k} \lambda_j \mathbf{e_j} \tag{9}$$

where λ_j are constants. If this is the case, $\mathbf{e}_i$ and π_i are removed from $\mathbf{Y}$ and $\boldsymbol{\pi}$, respectively, to obtain a new $\boldsymbol{\pi}$:

$$\boldsymbol{\pi} = \begin{bmatrix} \pi_1 (1+\lambda_1) \cdots \pi_{i-1} (1+\lambda_{i-1}) \pi_{i+1} (1+\lambda_{i+1}) \cdots \pi_k (1+\lambda_k) \end{bmatrix}^{\mathrm{T}} \tag{10}$$

This is an iterative procedure that terminates when no column $\mathbf{e_i}$ of $\mathbf{Y}$ can be written in the form of Eq. 10. Then, the final $\boldsymbol{\pi}$ contains the minimum set of estimated parameters. In such a case, the inverse of $\hat{\mathbf{Y}}^{\mathrm{T}} \hat{\mathbf{Y}}$ exists.

The system of equations, given by Eq. 4 is over-determined and the least-squares solution is,

$$\boldsymbol{\pi} = (\hat{\mathbf{Y}}^{\mathrm{T}} \hat{\mathbf{Y}})^{-1} \hat{\mathbf{Y}}^{\mathrm{T}} \hat{\mathbf{h}}_{\mathbf{CM}} \tag{11}$$

Once this vector is available, is enough to render system's full dynamics known, as required in model-based control.

3. SPACE EMULATORS

The complex tasks being performed in OOS missions demand on-earth planning and validation, leading to the need for laboratory emulation of the environment of space. The two main desired characteristics of space emulators are the elimination of the effect of gravitational forces in one or more planes and the free motion of the manipulator system without friction or other resisting forces. In order to achieve these, various solutions have been proposed including suspension systems, parabolic flights, neutral buoyancy underwater facilities and air-bearings test beds. Each solution has its own advantages and disadvantages [13]. As in other cases [14], the experimental facility designed and constructed at the NTUA's Control Systems Lab (CSL) is a planar robotic space emulator employing air-bearings.

4. THE NTUA CSL EMULATOR

The robotic space emulator of NTUA's Control Systems Lab (see "Fig. 3"), consists of a granite table, two autonomous robots, one of older ("Cassiopeia") and one of newer design ("Cepheus"), and an optical feedback system. The granite table has dimensions 2.2m x 1.8m x 0.3m, weighs approximately 3.5 tn and has very low surface roughness (smaller than 5μm) and very small inclination (smaller than 0.01°), thus allowing the simulation of frictionless microgravity conditions in two dimensions.

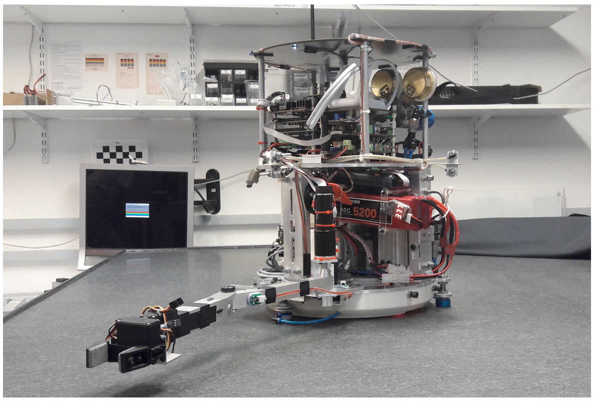

Figure 3. NTUA's Robotic Space Emulator "Cepheus".

The autonomous robot "Cepheus", (see "Fig. 4"), has a two-degrees-of-freedom manipulator mounted on an aluminium base, housing the various subsystems of the robot. Each joint of the arm controlled by a motor through a system of pulleys and belts. Both of the motors are placed on the main body of the robot, thus achieving a more desirable centre of mass of the system and are equipped with incremental encoders.

The suspension of the base above the granite table is achieved by three round air bearings, 25 mm in diameter, placed under the circular base and spaced at 120 degrees apart. Pressurized CO_2 is supplied through the porous material of the air bearings, thus creating a thin film of air (approximately 10 μm) between the base of the robot and the granite table, allowing frictionless planar motion. The CO_2 is provided to each of the three air bearings via flexible hoses from a central CO_2 tank placed near the centre of mass of the base, weighing 1500 gr (when full) under pressure 60 bar (at 20°C). The same tank provides the CO_2 necessary for the operation of the three pairs of thrusters, also placed peripherally

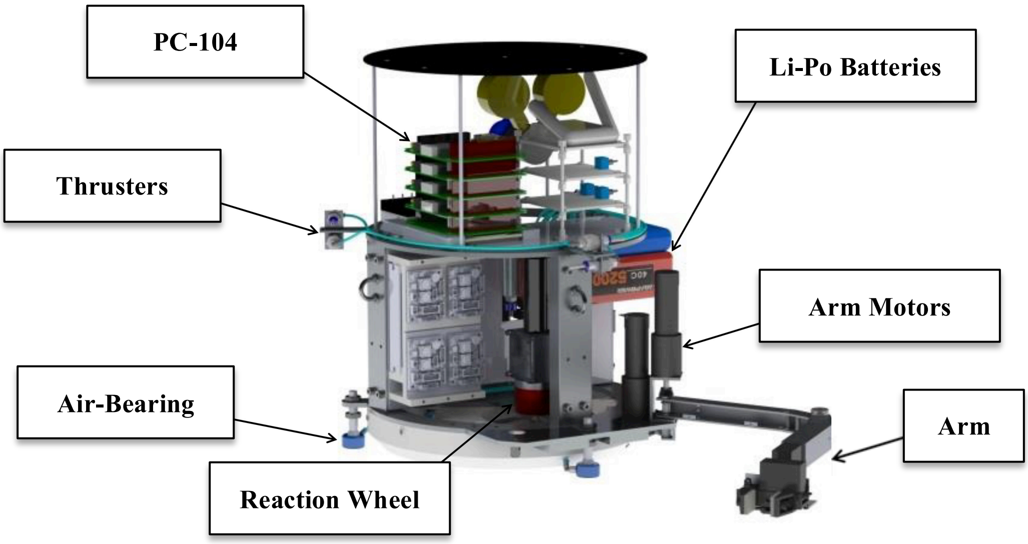

Figure 4. Parts of "Cepheus".

mid-height around the base at 120 degrees from each other. Each pair consists of two opposed thrusters controlled by 6 electric valves and therefore allowing control over the position and the attitude of the robotic system.

To achieve greater fuel (CO_2) autonomy, a reaction wheel installed. The rotation of the reaction wheel is controlled by a motor with an incremental encoder, offering an alternative to the thrusters for the attitude control of the robot. Moreover, the use of the reaction wheel makes the robot of the emulator resemble better an actual space robotic system, where the propulsion medium is limited in contrast to the practically infinite amount of electric energy available through the solar panels of the spacecraft.

The electrical autonomy of the robot is achieved by 2 Lithium Polymer (LiPo) batteries, with 4 cells each. The supply of the electric energy is being distributed in two independent circuits; one high voltage circuit suppling the 3 motors of the robot and the electric valves and one low voltage circuit supplying the computational subsystem of the robot. The energy conversion is conducted by two dc-dc converters, one for the high and one for the low voltage subsystem.

The computational system of the robot consists of 3 PC-104 boards and a Wi-Fi bridge. The operational system Ubuntu is installed in the PC-104 along with the open source software ROS (Robotic Operating System), which facilitates the control of the robot autonomously or via external PCs in collaboration with Matlab Simulink (MathWorks Inc.), see "Fig. 5".

Finally, the NTUA's planar emulator is equipped with a PhaseSpace system (8 cameras, LED drivers, LEDs, hub, server, and pre-wired calibration objects), placed around the granite table, for motion capturing and position feedback.

SIMULATION RESULTS

In this section, the proposed identification method is illustrated by the simulated NTUA's planar space emulator, although the method can be easily applied in spatial multi-arm FFSMS. The kinematic and inertia parameters of "Cepheus", obtained from CAD model, are given in "Tab. 1". The angular momentum of the system is set to $0.4934\,\text{Nms}$.

Table 1. Parameters of NTUA's "Cepheus".

Link i	l_i (m)	r_i (m)	m_i (kg)	I_{zz} (kg m^2)
0	-	$[0.17,0.09]^T$	9.951	0.1214
1	0.119	0.062	0.083	3.46e^{-4}
2	0.146	0.084	0.187	7.17e^{-4}

The developed exciting trajectories are based on truncated Fourier series. To satisfy desired initial and final conditions, a fifth-order polynomial is added to the truncated Fourier series:

$$q_i^{(m)} = \sum_{l=1}^{N_f} \frac{a_l^{(m)}}{\omega_f l} \sin\left(\omega_f l t\right) - \frac{b_l^{(m)}}{\omega_f l} \cos\left(\omega_f l t\right) + \sum_{j=0}^{5} c_j^{(m)} t^j \quad (12)$$

where $m = 1,\ldots n$, $i = 1,\ldots,N_m$, N_f is the number of the harmonics employed, $a_l^{i\,(m)}$ and $b_l^{i\,(m)}$ are free coefficients and $\omega_f = 2\pi/t_f$ with t_f the motion duration.

The free coefficients of the Fourier series are found by minimizing the condition number of the regressor matrix. The optimization algorithm is implemented using the Global Search Solver provided by the Global

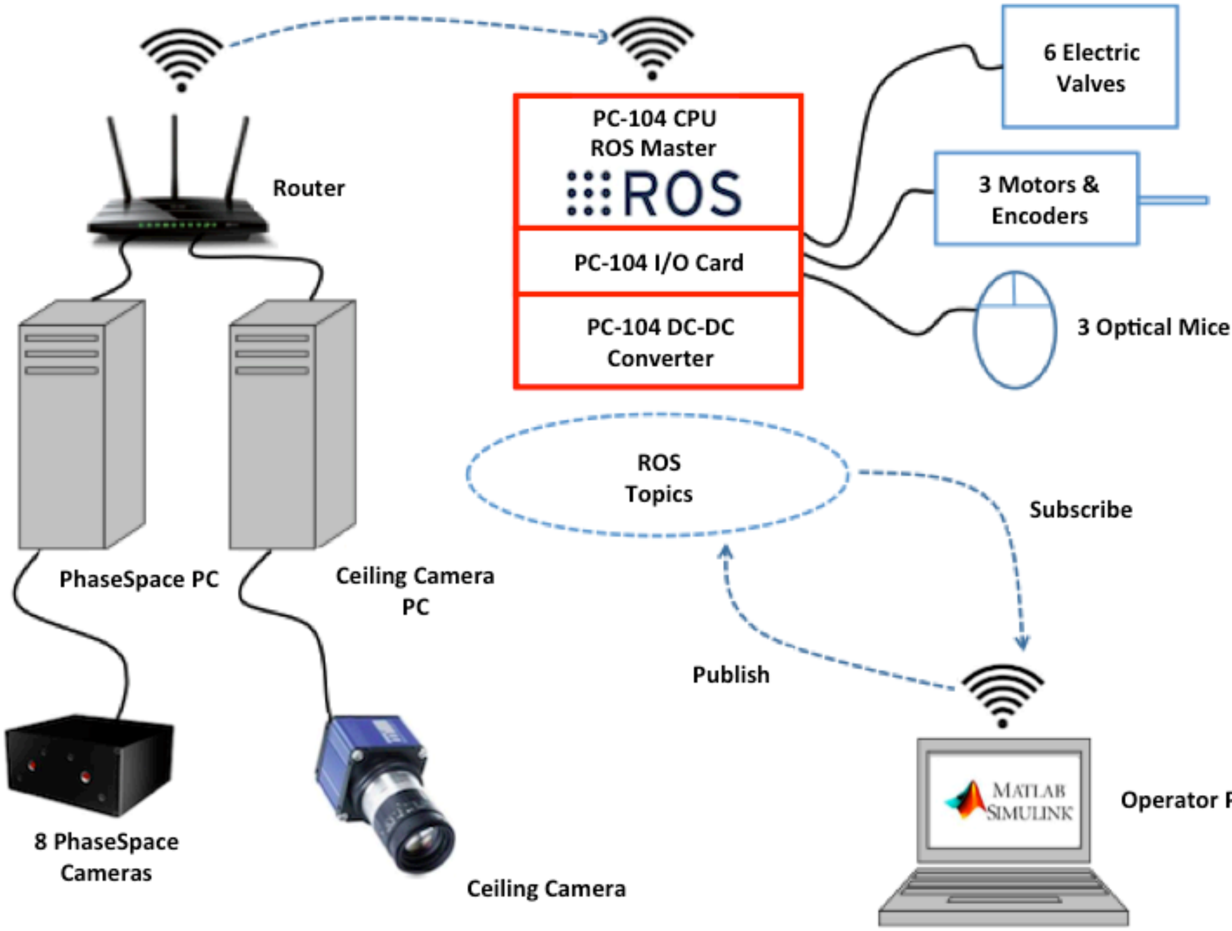

Figure 5. Robot Communication Schematic

Optimization Toolbox (MathWorks Inc.) taking into account mechanical constraints of space emulator on joint positions, velocities and accelerations.

In this simulation, $t_f = 5\,\mathrm{s}$ and $N_f = 3$. The desired initial and final conditions correspond to zero joint angles, rates and accelerations. The number of measurements is taken equal to $N = 35$. The coefficients a_l^i and b_l^i of the exciting trajectories are shown in "Tab. 2".

Table 2. Trajectory coefficients for minimum condition number

a_1^1	-0.1642	b_1^1	0.0010
a_2^1	0.2786	b_2^1	0.2090
a_3^1	0.3582	b_3^1	-0.1000
a_1^2	0.0846	b_1^2	0.3682
a_2^2	-0.1692	b_2^2	0.0597
a_3^2	0.0498	b_3^2	-0.32835

In the case of a planar 2-DOF manipulator system, the minimum set of estimated parameters is presented in APPENDIX B. The results of the proposed identification method are displayed in "Tab. 3". As shown in this table, the proposed method estimates the required parameters practically exactly, without the use of acceleration or joint torques. Moreover, these parameters are enough to reconstruct the system's full dynamics.

Table 3. Simulation results from the proposed method

π	π True value	Relative Error (%)
π_1	0.0074	0.5162
π_2	0.0046	0.4071
π_3	0.0039	0.3191
π_4	0.0024	1.2574
π_5	0.1314	0.0432
π_6	0.0048	0.7286
π_7	0.0075	1.3010
π_8	0.0046	0.6634

5. EXPERIMENT RESULTS

To conduct the experimental identification of NTUA's Space Emulator, angular momentum must be introduced to the system and then, appropriate exciting trajectories must be performed by the arm joints. During the arm motion, joint angles and base angular orientation are measured by the encoders and the PhaseSpace system, respectively. By differentiating these measurements with respect to time, joint rates and base angular velocity are obtained. Using N measurements of joint angles, joint rates and base angular velocity, the minimum set of parameters $\boldsymbol{\pi}$ is identified and the full dynamics of the space emulator is reconstructed.

To control the reaction wheel and the arm joints, ROS Control is used. The ros_control packages take as input the joint state data from the robot's actuator's encoders and an input set point. ROS Control uses a generic control loop feedback mechanism, typically a PID controller, to control the output, typically effort sent to actuators. There is a list of available controller plugins, contained in ros_controllers and in this experiment effort_controllers are used.

The experiment starts by setting the angular momentum of the system to a constant value using the reaction wheel. A PI velocity controller (effort_controllers/joint_velocity_controlller) for the reaction wheel is loaded in ROS and the desired relative velocity of the reaction wheel with respect to the base of the robot is published from Simulink at an external PC to the controller's ROS topic for velocity commands. The angular momentum of the system when the reaction wheel reaches the desired relative velocity is,

$$h_{CM} = I_{rw}\omega_{rw/des} \tag{13}$$

where I_{rw} is the reaction wheel moment of inertia about its symmetrical axis. Its value is known from CAD and equal to $I_{rw} = 0.00197372\,\text{kg}\cdot m^2$. In this experiment, the desired reaction wheel relative velocity is equal to $\omega_{rw/des} = 170$ rad/s. Therefore, $h_{cm} = 0.3355$ Nms.

Once "Cepheus" has constant angular momentum, the two joints of the arm start to perform the optimized exciting trajectories. A PD position controller (effort_controllers/joint_position_controlller) for each arm joint is loaded in ROS and the desired angle with respect to time for each joint is published from Simulink to the controller's ROS topic for position commands. In this experiment the exciting trajectories are sinusoidal and their duration is $t_f = 5\,\text{s}$. The number of measurements is taken equal to $N = 29$.

The proposed method identified the vector $\boldsymbol{\pi}$, i.e. the minimum set of estimated parameters required is available.

The experimentally identified parameters of NTUA's planar space emulator are sufficient for the complete dynamic reconstruction of the system. Therefore, one way to validate the experimental results and the success of the proposed identification method is to compare the dynamic response of the simulated system based on identified model of the space emulator-with the same angular momentum and same exciting trajectories as those applied to the hardware in the experiment- with the response of the hardware. The time histories of joint angles, joint rates and base angular velocity for both simulated system and hardware are shown in "Fig. 6". As shown in this figure, the time histories of joint angles and joint rates of the simulated identified system and the hardware coincide. However, concerning the base angular velocity, there is a small deviation between the simulation and the hardware. This may be due to the presence of friction between the air-bearings and the film of air.

6. CONCLUSIONS

In this paper, a novel parameter estimation method was developed, based on the conservation of the angular momentum of Free-Floating Space Manipulator Systems. The parameters to be identified are combinations of spacecraft, manipulator and payload parameters, and once available, they are enough to reconstruct the system full dynamics as required in model-based control. Only measurements of joint angles, rates, and spacecraft attitude and angular velocity are needed; noisy and hard to obtain spacecraft and manipulator joint accelerations or joint torques, are not required. Moreover, it does not require prior knowledge of any parameter and can be applied to free-floating systems with more than one manipulators. The effectiveness of the proposed method was validated by a numerical simulation. The main aspects NTUA's new planar robotic space emulator "Cepheus" have been presented and the identification method has been used for the experimental estimation of the system's dynamics.

7. AKNOWLEDGEMENTS

Olga Orsalia Christidi Loumpasefski was supported by an Onassis Foundation Scholarchip.

8. REFERENCES

1. Kelso, T.S. (2009). Analysis of the Iridium 33-Cosmos 2251 Collision. Paper AAS 09-368, American Astronautical Society. Paper AAS 09-368, American Astronautical Society. American Astronautical Society, Univelt, Escondido, Calif, USA.

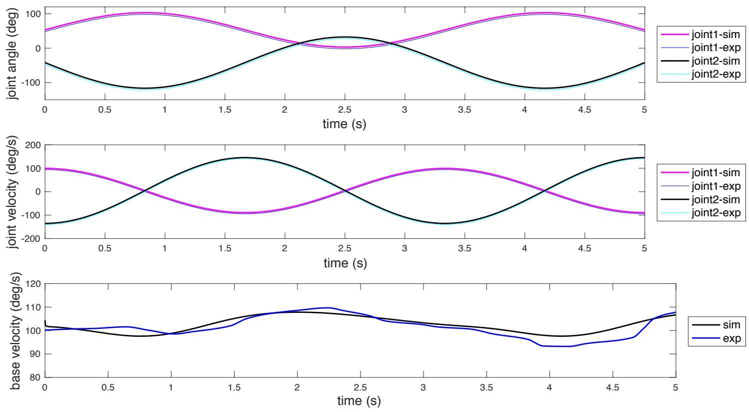

Figure 6. Responses of simulated space emulator based on identified model (sim) and hardware (exp)

2. Shan, M., Guo, J., and Gill, E. (2015). Progress in Aerospace Sciences Review and comparison of active space debris capturing and removal methods. *Prog. Aerosp. Sci.*, pp. 1–15.

3. Antonelli, G., Caccavale, F., and Chiacchio, P. (1999). A systematic Procedure for Identification of Dynamic Parameters of Robot Manipulators. *Robotica,* Vol. 17, 1999, pp. 427–435.

4. Atkeson, C. G., An, C. H., and Hollerbach, J. M. (1994). Estimation of Inertial Parameters of Manipulator Loads and Links. *Journal of Guidance, Control, and Dynamics,* Vol. 17, No. 3, pp. 488–494.

5. Shin, J.-H., and Lee, J.-J. (1994). Dynamic control with adaptive identification for free-flying space robots in joint space. *Robotica,* Vol. 12, pp. 541–551.

6. Wang, H., and Xie, Y. (2012). Prediction Error Based Adaptive Jacobian Tracking for Free-Floating Space Manipulators. *IEEE Tr. on Aerospace and Electronic Systems,* Vol. 48, No.4, pp. 3207-3221.

7. Yoshida, K., and Abiko, S. (2002). Inertia Parameter Identification for a Free-Flying Space Robot. *Proc. AIAA Guidance, Navigation and Control,* Monterey, CA.

8. Ma, O., and Dang, H. (2008). On-Orbit Identification of Inertia Properties of Spacecraft Using a Robotic Arm. *Journal of Guidance, Control, and Dynamic*, Vol. 31, No. 6, pp. 1761–1771.

9. Murotsu, Y., Senda, K., Ozaki, M., and Tsujio, S. (1994). Parameter Identification of Unknown Object Handled by Free-Flying Space Robot. *Journal of Guidance, Control, and Dynamics*. Vol. 17, No. 3, pp. 488–494.

10. Christidi-Loumpasefski, O.-O., Nanos, K., and Papadopoulos, E. (2017). On Parameter Estimation of Space Manipulator Systems Using the Angular Momentum Conservation. *Proc. IEEE International Conference on Robotics and Automation (ICRA '17)*, Singapore.

11. Dubowsky, S. and Papadopoulos E. (1993). The kinematics, Dynamics, and Control of Free-Flying and Free-Floating Space Robotic Systems. *IEEE Transactions on Robotics and Automation,* Vol. 9, No. 5, pp. 531-543.

12. Nanos, K., and Papadopoulos, E. (2011). On the Use of Free-floating Space Robots in the Presence of Angular Momentum. *Intelligent Service Robotics, Sp. Issue on Space Robotics,* Vol. 4, No. 1, pp. 3-15.

13. Menon, C., Busolo, S., Cocuzza, S., Aboudan, A., Bulgarelli, A., Bettanini, C., Marchesi, M., and Angrilli, F. (2007). Issues and solutions for testing free-flying robots. 60, pp. 957–965.

14. Miller, D., Wertz, J., Chen, A., Berkowski, G., and Brodel, C. (2000). SPHERES : A Testbed For Long Duration Satellite Formation Flying In Micro-Gravity Conditions."

15. Moosavian, S. Ali A., Papadopoulos, E. (2004). Explicit Dynamics of Space Free-Flyers with Multiple Manipulators via SPACEMAPLE. *Advanced Robotics,* Vol. 18 , No. 2, pp. 223-244.

APPENDIX A

The matrices ${}^{0}\mathbf{D}$, ${}^{0}\mathbf{D}_{\mathbf{q}}$ and ${}^{0}\mathbf{D}_{\mathbf{qq}}$, expressed in the spacecraft frame, are presented.

First, the term ${}^{0}\mathbf{D}$ is given by,

$$ {}^{\mathbf{0}}\mathbf{D} = {}^{\mathbf{0}}\mathbf{D}_{\mathbf{0}} + \sum_{m=1}^{n}\sum_{j=1}^{N_m} {}^{\mathbf{0}}\mathbf{D}_{\mathbf{j}}^{(m)} \tag{A1} $$

where

$$ \begin{aligned} {}^{\mathbf{0}}\mathbf{D}_{\mathbf{0}} = {}& {}^{\mathbf{0}}\mathbf{I}_{\mathbf{0}} + \sum_{m=1}^{n}\sum_{i=1}^{Nm} {}^{\mathbf{0}}\mathbf{D}_{\mathbf{i0}}^{(m)} + \sum_{m=1}^{n} \frac{M\sum_{k=1}^{Nm} m_k^{(m)}}{M-\sum_{k=1}^{N_m} m_k^{(m)}} [{}^{\mathbf{0}}\tilde{\mathbf{r}}_{\mathbf{0}}^{(m)}, {}^{\mathbf{0}}\tilde{\mathbf{r}}_{\mathbf{0}}^{(m)}] \\ & - \sum_{m=1}^{n}\sum_{\substack{q=1\\ q\neq m}}^{n} \frac{M\sum_{k=1}^{Nm} m_k^{(m)} \sum_{k=1}^{Nq} m_k^{(q)}}{\left(M-\sum_{k=1}^{N_m} m_k^{(m)}\right)\left(M-\sum_{k=1}^{Nq} m_k^{(q)}\right)} [{}^{\mathbf{0}}\tilde{\mathbf{r}}_{\mathbf{0}}^{(m)}, {}^{\mathbf{0}}\tilde{\mathbf{r}}_{\mathbf{0}}^{(q)}] \\ & + \sum_{m=1}^{n}\sum_{\substack{q=1\\ q\neq m}}^{n}\sum_{i=1}^{N_q} \frac{M\sum_{k=1}^{Nm} m_k^{(m)}}{M-\sum_{k=1}^{N_m} m_k^{(m)}} [{}^{\mathbf{0}}\tilde{\mathbf{r}}_{\mathbf{0}}^{(m)}, {}^{\mathbf{0}}\tilde{\mathbf{l}}_{\mathbf{i}}^{(q)}] \end{aligned} \tag{A2} $$

and

$$ \begin{aligned} {}^{\mathbf{0}}\mathbf{D}_{\mathbf{j}}^{(m)} = {}& \sum_{i=0}^{N_m} {}^{\mathbf{0}}\mathbf{D}_{\mathbf{ij}}^{(m)} - \sum_{\substack{q=1\\ q\neq m}}^{n}\sum_{k=1}^{N_q} M[{}^{\mathbf{0}}\tilde{\mathbf{l}}_{\mathbf{j}}^{(m)}, {}^{\mathbf{0}}\tilde{\mathbf{l}}_{\mathbf{k}}^{(q)}] \\ & + \sum_{\substack{q=1\\ q\neq m}}^{n} \frac{M\sum_{k=1}^{N_q} m_k^{(q)}}{M-\sum_{k=1}^{N_q} m_k^{(q)}} [{}^{\mathbf{0}}\tilde{\mathbf{l}}_{\mathbf{j}}^{(m)}, {}^{\mathbf{0}}\tilde{\mathbf{r}}_{\mathbf{0}}^{(q)}] \end{aligned} \tag{A3} $$

where

$$ {}^{\mathbf{0}}\mathbf{D}_{\mathbf{ij}}^{(m)} = \begin{cases} -M[{}^{\mathbf{0}}\tilde{\mathbf{l}}_{\mathbf{j}}^{(m)}, {}^{\mathbf{0}}\tilde{\mathbf{r}}_{\mathbf{i}}^{(m)}] & i<j \\ {}^{\mathbf{0}}\mathbf{I}_{\mathbf{i}}^{(m)} + m_i^{(m)}[{}^{\mathbf{0}}\tilde{\mathbf{e}}_{\mathbf{i}}^{(m)}, {}^{\mathbf{0}}\tilde{\mathbf{e}}_{\mathbf{i}}^{(m)}] + m_0[{}^{\mathbf{0}}\tilde{\mathbf{l}}_{\mathbf{i}}^{(m)}, {}^{\mathbf{0}}\tilde{\mathbf{l}}_{\mathbf{i}}^{(m)}] & \\ +\left(\sum_{\substack{q=1\\ q\neq m}}^{n}\sum_{k=1}^{N_q} m_k^{(q)} + m_1^{(m)} + \ldots + m_{i-1}^{(m)}\right)[{}^{\mathbf{0}}\tilde{\mathbf{l}}_{\mathbf{i}}^{(m)}, {}^{\mathbf{0}}\tilde{\mathbf{l}}_{\mathbf{i}}^{(m)}] & i=j \\ +(m_{i+1}^{(m)} + \ldots + m_{N_m}^{(m)})[{}^{\mathbf{0}}\tilde{\mathbf{r}}_{\mathbf{i}}^{(m)}, {}^{\mathbf{0}}\tilde{\mathbf{r}}_{\mathbf{i}}^{(m)}] & \\ -M[{}^{\mathbf{0}}\tilde{\mathbf{r}}_{\mathbf{j}}^{(m)}, {}^{\mathbf{0}}\tilde{\mathbf{l}}_{\mathbf{i}}^{(m)}] & i>j \end{cases} \tag{A4} $$

The term ${}^{\mathbf{0}}\mathbf{D}_{\mathbf{q}}$ is given by,

$$ {}^{\mathbf{0}}\mathbf{D}_{\mathbf{q}} = \left[\, {}^{\mathbf{0}}\mathbf{D}_{\mathbf{q}}^{(1)} \quad \cdots \quad {}^{\mathbf{0}}\mathbf{D}_{\mathbf{q}}^{(m)} \quad \cdots \quad {}^{\mathbf{0}}\mathbf{D}_{\mathbf{q}}^{(n)} \,\right] \tag{A5} $$

where

$$ {}^{\mathbf{0}}\mathbf{D}_{\mathbf{q}}^{(m)} = \sum_{j=1}^{N_m} {}^{\mathbf{0}}\mathbf{D}_{\mathbf{j}}^{(m)}\ {}^{\mathbf{0}}\mathbf{F}_{\mathbf{j}}^{(m)} \tag{A6} $$

and

$$ {}^{\mathbf{0}}\mathbf{F}_{\mathbf{j}}^{(m)} = \left[\, {}^{\mathbf{0}}\mathbf{z}_{\mathbf{1}}^{(m)} \quad \cdots \quad {}^{\mathbf{0}}\mathbf{z}_{\mathbf{j}}^{(m)} \quad \cdots \quad \mathbf{0}_{3\times(\mathrm{N}_m-\mathrm{j})} \,\right] \tag{A7} $$

where ${}^{\mathbf{0}}\mathbf{z}_{\mathbf{j}}^{(m)}$ is the unit vector along the j-th joint's axis of the m-th manipulator expressed in spacecraft frame and $\mathbf{0}$ is the zero matrix.

In Eqs. A2–A4, the body-fixed barycentric vectors ${}^{\mathbf{0}}\tilde{\mathbf{l}}_{\mathbf{k}}^{(m)}$, ${}^{\mathbf{0}}\tilde{\mathbf{r}}_{\mathbf{k}}^{(m)}$ and ${}^{\mathbf{0}}\tilde{\mathbf{e}}_{\mathbf{k}}^{(m)}$ are given in [15] and

$$ [\mathbf{a},\mathbf{b}] = (\mathbf{a}\cdot\mathbf{b})\mathbf{1} - \mathbf{ab} \tag{A8} $$

where $\mathbf{1}$ is the unit dyadic.

APPENDIX B

In the case of a planar 2-DOF manipulator system the minimum set of estimated parameters, i.e. the elements of the $\boldsymbol{\pi}$ vector are shown below:

$$ \pi_1 = \frac{m_0}{m_0+m_1+m_2} r_{0x}\left(l_1\left(m_1+m_2\right)+m_2 r_1\right) \tag{B1} $$

$$ \pi_2 = \frac{l_2 m_0 m_2}{m_0+m_1+m_2} r_{0x} \tag{B2} $$

$$ \pi_3 = \frac{m_0}{m_0+m_1+m_2} r_{0y}\left(l_1\left(m_1+m_2\right)+m_2 r_1\right) \tag{B3} $$

$$ \pi_4 = \frac{l_2 m_0 m_2}{m_0+m_1+m_2} r_{0y} \tag{B4} $$

$$ \pi_5 = I_0 + \frac{m_0\left(m_1+m_2\right)}{m_0+m_1+m_2}\left(r_{0x}^2+r_{0y}^2\right) \tag{B5} $$

$$ \pi_6 = \frac{l_2 m_2}{m_0+m_1+m_2}\left(l_1 m_0 + \left(m_0+m_1\right) r_1\right) \tag{B6} $$

$$ \pi_7 = I_1 + \frac{l_1^2 m_0\left(m_1+m_2\right) + 2 l_1 m_0 m_2 r_1 + \left(m_0+m_1\right) m_2 r_1^2}{m_0+m_1+m_2} \tag{B7} $$

$$ \pi_8 = I_2 + \frac{l_2^2\left(m_0+m_1\right) m_2}{m_0+m_1+m_2} \tag{B8} $$